Impact of Textile on Electromagnetic Power and Heating in Near-Surface Tissues at 26 GHz and 60 GHz

Giulia Sacco, *Student Member, IEEE*, Stefano Pisa, *Senior Member, IEEE*, and Maxim Zhadobov, *Senior Member, IEEE*

***Abstract*—With the development of 5th generation (5G) networks the operating frequencies have been progressively expanding towards millimeter waves (MMW). In some exposure scenarii, presence of textiles impacts the interaction of the electromagnetic field radiated by wireless devices with human tissues. We investigate the impact of a textile layer in contact or in proximity of skin on the power transmission coefficient, absorbed power density and temperature rise using a near-surface tissue model at 26 GHz and 60 GHz. Cotton and wool are considered as representative textiles. Our results demonstrate that the textile in contact with skin increases the absorbed power density up to 41.5% at 26 GHz and 34.4% at 60 GHz. The presence of an air gap between a textile and skin modifies the electromagnetic power deposition in the tissues depending on the thicknesses and permittivity. The temperature rise increases compared to the bare skin by up to 52% at 26 GHz and 46% at 60 GHz with the textile in direct contact with skin. With an air gap, for typical textile thicknesses, the temperature variations range from −3.5% to 20.6% and from −11.1% to 20.9% at 26 GHz and 60 GHz, respectively.**

***Index Terms*—5G, millimeter waves (MMW), textile, electromagnetic and thermal dosimetry.**

I. Introduction

RECENT advances in millimeter waves (MMW) technologies together with the growing need for high data rates and secure communications are leading to the fast development of 5th generation (5G) mobile networks, whose operating frequencies have been progressively shifting towards the MMW band [1], [2].

Exposure guidelines have been defined by the International Commission on Non-Ionizing Radiation Protection (ICNIRP) and Institute of Electrical and Electronics Engineers (IEEE) [3], [4]. In the 6 GHz–300 GHz range, exposure limits are expressed in terms of the incident power density (IPD), whose value for whole body exposure should be limited to 10 W m^{-2} and 50 W m^{-2} (averaged over 30 min) for unrestricted environment/general public exposure and restricted environment/occupational exposure, respectively. For local exposures, frequency-dependent limits are recommended, i.e. the IPD should not exceed $55 f_G^{-0.177}$ (f_G: frequency in GHz) for unrestricted environment/general public exposure and $275 f_G^{-0.177}$ or $274.8 f_G^{-0.177}$ for restricted environment/occupational exposure according to ICNIRP and IEEE, respectively [3], [4]. The IPD values should be averaged over 4 cm^2 and 6 min. To account for a smaller beam diameter above 30 GHz, the IPD averaged over 1 cm^2 is allowed to exceed the limit by a factor of 2.

Recent studies investigated the exposure under realistic conditions with the user terminal close to the head [5], focusing on thermoregulation [6] or on the impact of pulsed fields [7], [8]. At MMW, the interaction between human tissues and the incident electromagnetic field in terms of the deposited power and resulting heating was investigated in several works [9]–[11]. All these studies consider the electromagnetic field impinging directly on the bare skin. However, in some use cases, clothing can modify the electromagnetic power absorption in tissues and resulting temperature rise. A representative example is when, during a call, the user places the phone in his pocket while using a headphone. Other possible scenarii include the usage of a tablet lying on the user's legs or of radiating devices during wintertime, when wearing hats or gloves. In all these conditions, the presence of textiles is to be taken into account for accurate dosimetry.

Several studies considered the impact of clothes at MMW [12]–[15]. In particular, [15] investigated how the presence of a textile layer affects the power transmission coefficient, demonstrating that the clothing can act as an impedance transformer and increase the absorption. Body-centric propagation in the context of the body area networks at 60 GHz was investigated in [12]–[14] in term of the path gain. These studies analysed the power transmission coefficient in presence of a textile on simplified model of skin, without considering the deposited electromagnetic power and the resulting heating, which may also be impacted by the subcutaneous fat and muscle [11].

The main purpose of this study is to investigate analytically and numerically the electromagnetic power deposition and

Manuscript received September 22, 2020; revised November 17, 2020; accepted November 27, 2020. Date of publication December 3, 2020; date of current version August 21, 2021. The work was supported by the French National Research Program for Environmental and Occupational Health of ANSES under Grant 2018/2 RF/07 through NEAR 5G project. *(Corresponding author: Giulia Sacco.)*

Giulia Sacco is with the Department of Information Engineering, Electronics and Telecommunications, Sapienza University of Rome, Rome 00184, Italy, and also with the University Rennes, CNRS, Institut d'Électronique et des Technologies du numéRique (IETR), F-35000 Rennes, France (e-mail: giulia.sacco.it@gmail.com).

Stefano Pisa is with the Department of Information Engineering, Electronics and Telecommunications, Sapienza University of Rome, Rome 00184, Italy (e-mail: stefano.pisa@uniroma1.it).

Maxim Zhadobov is with the University Rennes, CNRS, IETR (Institut d'Électronique et des Technologies du numéRique), F-35000 Rennes, France (e-mail: maxim.zhadobov@univ-rennes1.fr).

Digital Object Identifier 10.1109/JERM.2020.3042390

TABLE I
PERMITTIVITY, THERMAL CONDUCTIVITY, MASS DENSITY, AND BLOOD PERFUSION OF THE MODEL LAYERS

Layer	ε^*		λ_i (W m^{-1} °C^{-1})	ρ_i (kg m^{-3})	B_i (W m^{-3} °C^{-1})
	26 GHz	60 GHz			
stratum corneum (SC)	$3.62 - j0.74$	$3.15 - j0.50$	0.37	1500	0
Viable epidermis	$17.71 - j16.87$	$7.98 - j10.90$	0.37	1109	0
Dermis	$17.71 - j16.87$	$7.98 - j10.90$	0.37	1109	7440
Fat	$3.76 - j1.10$	$3.13 - j0.84$	0.21	911	1900
Muscle	$25.85 - j21.84$	$12.86 - j15.83$	0.49	1090	2550
Air	1		0.027	1.13	0
Cotton	$2 - j0.04$		0.071	500	0
Wool	$1.22 - j0.036$		0.054	500	0

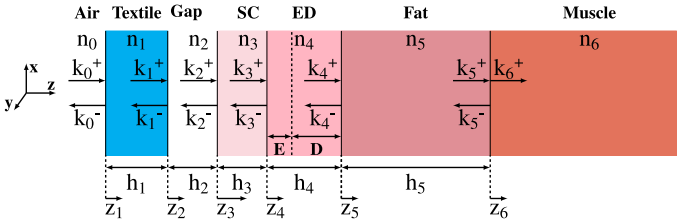

Fig. 1. Model used for calculation of absorbed power and temperature rise.

consequent temperature rise in a near-surface multilayer tissue model considering the impact of a textile layer on or in vicinity of skin. Cotton and wool, two textile materials typically used for clothes realization, are employed as representative models. The analysis is performed at 26 GHz and 60 GHz, frequencies upcoming for 5G and future generations of wireless technologies. For the sake of simplicity and brevity, we refer to 26 GHz as MMW, since at this frequency the interactions between the human tissues and electromagnetic fields are similar to the ones at lower frequencies of the MMW band.

II. MATERIALS AND METHODS

A near-surface tissue model illuminated by a normal impinging plane wave is used to assess the electromagnetic power deposition and resulting heating in presence of a textile (Fig. 1). Two configurations are considered: (1) clothes in contact with skin (1 with $h_2 = 0$ mm), and (2) clothes in proximity of the biological tissues in presence of an air gap between the textile material and skin ($h_2 > 0$ mm). The tissue model consists of 4 layers: stratum corneum (SC), viable epidermis and dermis (ED), fat, and muscle. The SC is the uppermost layer of the epidermis and is characterized by a low water content (roughly 2% by weight [11]) and typical thickness of 10μm–20μm [16]. The ED layer is composed of the remaining portion of the epidermis and dermis. The latter, has almost the same water content as viable epidermis and therefore, from the electromagnetic point of view, can be considered as the same layer. However, since only dermis contains blood vessels, epidermis and dermis are considered as two separate layers for the thermal analysis. As at MMW the penetration depth is limited to skin, fat and muscle layers almost do not affect the electromagnetic field distribution but they impact the temperature rise.

The complex permittivity ε^* of the considered model is reported in Table I. The permittivity of SC is taken from [11], while the ones of the remaining layers (ED, fat and muscle) correspond to the dry skin, not-infiltrated fat and muscle in [17]. Cotton and wool, with the thickness ranging from 0 mm to 3 mm (typical values are 0.2 mm for cotton and 2 mm for wool [14]), have been considered as representative textiles. Their permittivity measured at 60 GHz was reported in [14]. The textiles are assumed to be non-dispersive in the frequency range considered in this study [18], [19]. The power transmission coefficient, absorbed (or epithelial) power density [3], [4], referred hereafter as PD, and maximal temperature elevation in the skin layer were analytically calculated and numerically computed considering the IPD limits for whole body exposure and the frequency dependent ones (30.90 W m^{-2} and 26.65 W m^{-2} at 26 GHz and 60 GHz, respectively). The power transmission coefficient is computed at the interface between the textile and the surrounding environment as $|T|^2 = 1 - |R_0|^2$, where R_0 is the reflection coefficient between air and the textile layer. The PD is defined as the power flow through the SC per unit area on the body surface [3], [4]. Note that for the considered planar model and continuous plane-wave illumination, spatial or temporal averaging would not change the results since the PD is invariant in time and uniform in the x and y directions.

A. Analytical Model

The electromagnetic problem for a multilayer model excited by a plane wave can be solved analytically. Hypothesizing a normal wave incidence, the wave vector is directed along z, while the electric field is along x axis. Assuming that the power transmitted to the muscle layer from fat is entirely dissipated, the total electric field $E_i(z_i)$ in the i$_{\text{th}}$ layer is given by

$$E_i(z_i) = E_0^+ \times \frac{e^{jk_i(h_i - z_i)}\left(1 + R_i e^{-j2k_i(h_i - z_i)}\right)}{\prod_{n=0}^{i-1} \frac{1}{1+r_n} e^{jk_{n+1}h_{n+1}}\left(1 + r_n R_{n+1} e^{-j2k_{n+1}h_{n+1}}\right)}, \quad (1)$$

where $R_i = E_i^-/E_i^+$ is the reflection coefficient at the i_{th} interface, $r_i = (n_i - n_{i+1})/(n_i + n_{i+1})$ is a function of $n_i = \sqrt{\varepsilon_i^*}$, and k_i is the wave number in the i_{th} layer. For the textile in direct contact with skin, the subscripts exceeding 2 are reduced by 1. From the root mean square value of the electric field $E_{i_{rms}}$, conductivity σ_i and density ρ_i, the specific absorption rate (SAR) is calculated as:

$$SAR_i = \frac{\sigma_i \left|E_{i_{rms}}\right|^2}{\rho_i}. \quad (2)$$

Using SAR as a heat source, the temperature rise can be computed from the bioheat equation

$$\lambda_i \frac{d^2 T_i(z_i)}{dz_i^2} = B_i \left(T_i(z_i) - T_{blood}\right) - \rho_i SAR_i(z_i) \ , \quad (3)$$

where $T_{blood} = 37$ °C is the blood temperature, λ_i is the thermal conductivity of the i_{th} layer, $B_i = BF_i \rho_b C_b$ is the blood perfusion that depends on the volumetric blood flow rate of the i_{th} layer BF_i, on the blood density $\rho_b = 1050$ kg m $^{-3}$ and on the heat capacity $C_b = 3617$ J kg^{-1} ° C^{-1} [20]. Metabolic heat was neglected since the temperature rise rather than its absolute value was considered. The thermal conductivity, mass density, and blood perfusion are summarized in Table I. The thermal conductivities and densities of the ED, fat, and muscle are taken from [20]. The thermal conductivity, blood flow and mass density for the biological tissues are taken from [9]. The thermal conductivity of the textile materials are from [21]. The mass density of the textiles $\rho_{textile} = 500$ kg m^{-3} represents a typical value [21], [22].

The temperature distribution in the tissue layers is obtained solving Equation 3. In absence of an air gap between textile and skin ($h_2 = 0$ mm in Figure 1), the continuity of the temperature and heat flux at the interface between two intermediate layers is imposed:

$$T_i(h_i) = T_{i+1}(0) \quad (4)$$

$$-\lambda_i \left.\frac{dT_i(z_i)}{dz_i}\right|_{z_i=h_i} = -\lambda_{i+1} \left.\frac{dT_{i+1}(z_{i+1})}{dz_{i+1}}\right|_{z_{i+1}=0} , \quad (5)$$

while the boundary conditions for the deepest and the uppermost layer are

$$T_{last}(\infty) = T_{blood} \quad (6)$$

$$-\left.\frac{dT_1(z_1)}{dz_1}\right|_{z_1=0} = \frac{h}{\lambda_1}\left(T_1(0) - T_{air}\right) , \quad (7)$$

respectively. The heat transfer coefficient h between the textile and surrounding environment is set to 5 W m $^{-1}$ ° C^{-1} [23]. The study is performed at the ambient temperature $T_{air} = 20$ °C. The same boundary conditions apply to the configuration with an air gap between the textile and skin, except for the interface 1 and 2. The presence of an air gap between the textile and skin can be treated as a closed enclosure [16], [24], [25], and the heat flux at its boundaries can be described as

$$-\lambda_1 \left.\frac{dT_1(z_1)}{dz_1}\right|_{z_1=h_{Textile}} = Nu \frac{\lambda_{air}}{h_{gap}} \left(T_3(0) - T_1(h_{textile})\right) , \quad (8)$$

$$-\lambda_3 \left.\frac{dT_3(z_3)}{dz_3}\right|_{z_3=0} = Nu \frac{\lambda_{air}}{h_{gap}} \left(T_3(0) - T_1(h_{textile})\right) , \quad (9)$$

where Nu is the Nusselt number, h_{gap} is the gap thickness and λ_{air} is the air thermal conductivity [26] at 37 °C. Below the exposure limits [3], [4], the temperature rise in the human tissues is expected not to exceed 1 °C, and therefore convection inside the air gap is neglected. In this case, the heat exchange in the air gap is reduced to conductivity and $Nu = 1$ [27].

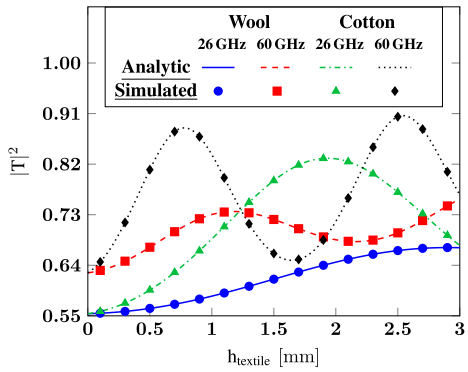

Fig. 2. Power transmission coefficient at 26 GHz and 60 GHz in presence of a textile layer in contact with skin.

B. Numerical Model

A stratified model analogous to the one presented in Fig. 1 was simulated using a finite element method. The layers properties are the same as the ones used in the analytical model, except for the muscle thickness, supposed infinite in the analytical analysis and set to 60 mm in simulations. A perfect electric conductor was used at the boundaries perpendicular to the E field (y direction) and Floquet periodic boundary conditions in the x direction. An excitation and an observation port were located in the z direction at the top and bottom boundaries, respectively. For the thermal analysis, adiabatic boundaries were imposed in the x and y directions, while the temperature at the deepest extremity of the muscle was set to 37 °C. At the interface between the textile and air the same condition as in (7) was imposed.

III. Results

A. Power Transmission Coefficient

The two parameters affecting the transmission at the air/textile interface when the textile is in direct contact with skin are its thickness and permittivity. Fig. 2 reports the power transmission coefficient in presence of cotton or wool.

The transmission increases compared to the air/skin interface without textile. An oscillatory behaviour is observed since, at certain thicknesses, the textile acts as a matching layer (e.g. for cotton 1.93 mm and 2.54 mm at 26 GHz and 60 GHz, respectively). The absorbed power is the highest when the textile has a thickness close to $(2n+1)\lambda/4$, with λ the wavelength in the material and n an integer. In particular, $\lambda/4$ at 26 GHz corresponds to 2.61 mm for wool and to 2.04 mm for cotton. At 60 GHz, it is equal to 1.13 mm and 0.88 mm for wool and cotton, respectively. The maximum power transmission coefficient does not occur exactly at these thicknesses. This can be attributed to the fact that, contrary to an ideal quarter-wave impedance transformer, the impedance of the textile is fixed by the material and is in general different from the one assuring the optimal matching conditions. Depending on the textile thickness, at 26 GHz the power transmission coefficient varies from about 55% ($h_2 = 0$ mm) to 67% ($h_2 = 2.91$ mm) for wool and from 55% to 83% ($h_2 = 1.93$ mm) for cotton. At 60 GHz, it is between

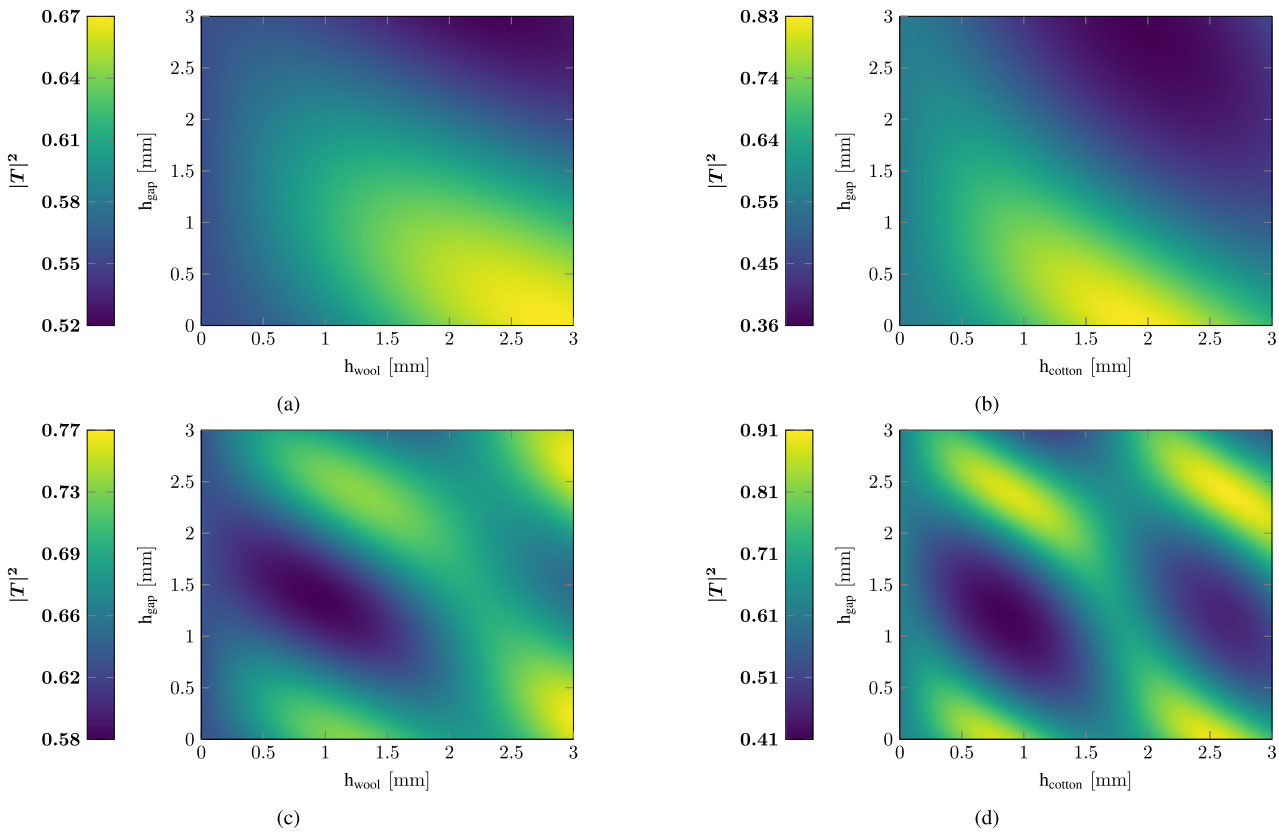

Fig. 3. Power transmission coefficient at 26 GHz: (a) with wool and (b) with cotton, and at 60 GHz: (c) with wool and (d) with cotton.

63% ($h_2 = 0$ mm) and 76% ($h_2 = 3$ mm) for wool and between 63% and 91% ($h_2 = 2.54$ mm) for cotton.

When the textile is separated from skin by an air gap, concurrently with the textile thickness and permittivity, the air gap thickness impacts the power transmission coefficient. A parametric study was performed to analyse the sensitivity of the power transmission coefficient to the textile and air gap thicknesses in presence of wool and cotton (Fig. 3). At 26 GHz, the maximum transmission is observed for $h_{gap} = 0$ mm, $h_{wool} = 2.91$ mm and $h_{gap} = 0$ mm, $h_{cotton} = 1.93$ mm. At 60 GHz, for each textile, local maxima appear for four different combinations of h_{gap} and $h_{textile}$. For wool the peak transmission (77%) occurs in two different conditions: $h_{gap} = 0.22$ mm, $h_{wool} = 3$ mm and $h_{gap} = 2.72$ mm, $h_{wool} = 3$ mm. For cotton, four different combinations of textile and air gap thickness ($h_{gap} = 0$ mm and $h_{cotton} = 0.78$ mm or $h_{cotton} = 2.54$ mm, and $h_{gap} = 2.39$ mm and $h_{cotton} = 0.90$ mm or $h_{cotton} = 2.66$ mm) assure the highest power transmission coefficient (91%). Note that, as the reflection coefficient at the air/skin interface decreases due to the presence of a textile, the performances of a wireless device placed in vicinity of the body may change compared to the exposure scenario without textile [5], [28].

B. Absorbed Power Density

Fig. 4 shows the PD in presence of a textile in contact with skin. As for the power transmission coefficient, PD increases in presence of the textile and shows an oscillatory behavior as a function of the textile thickness. The maximal PD is observed for a cotton layer with a thickness close to $\lambda/4$ at 60 GHz (34.4% increase compared to the case without textile). At 60 GHz, two local maxima appear for cotton close to $h_{textile} = \lambda/4$ and $h_{textile} = 3/4\lambda$. While for these two thicknesses the power transmission coefficient is almost the same, the corresponding PD decreases when the textile thickness increases. This can be attributed to higher losses in textile for $h_{textile} = 3/4\lambda$. At 26 GHz, the highest PD is observed for 1.84 mm thick cotton (7.83 W m^{-2} for $IPD = 10$ W m^{-2} and 24.20 W m^{-2} for

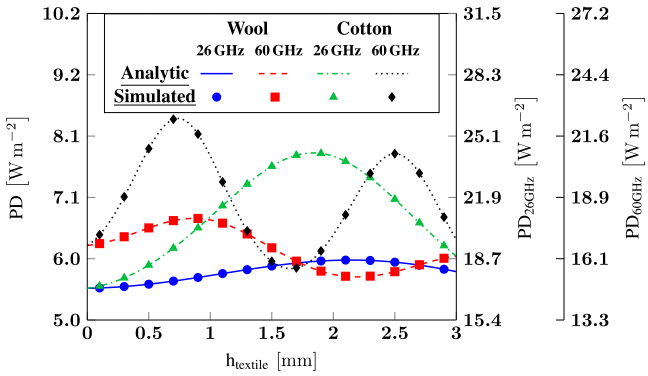

Fig. 4. Absorbed power density in presence of a textile layer in contact with skin. The left y axis refers to the frequency-independent IPD limits, while the two y axis on the right refer to the IPD frequency-dependent limits.

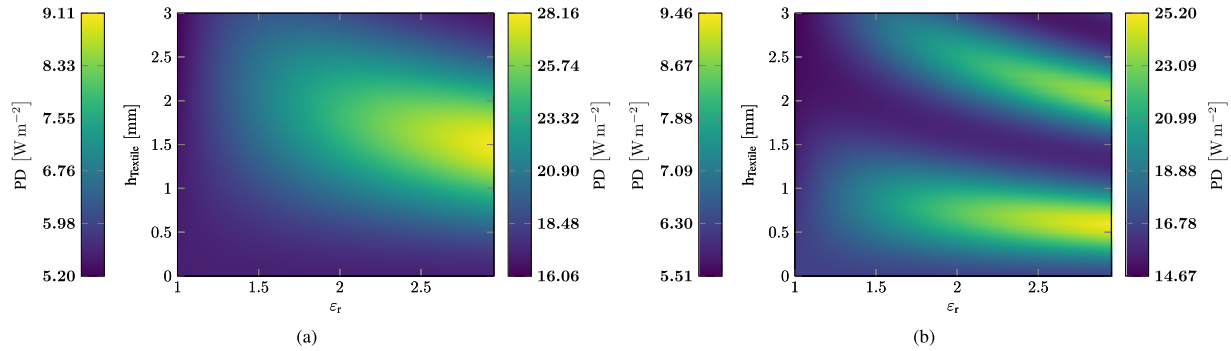

Fig. 5. Absorbed power density as a function of the textile thickness and real permittivity ε_r (a) at 26 GHz and (b) at 60 GHz. The left and right colorbars refer to the frequency-independent and frequency-dependent limits of IPD, respectively.

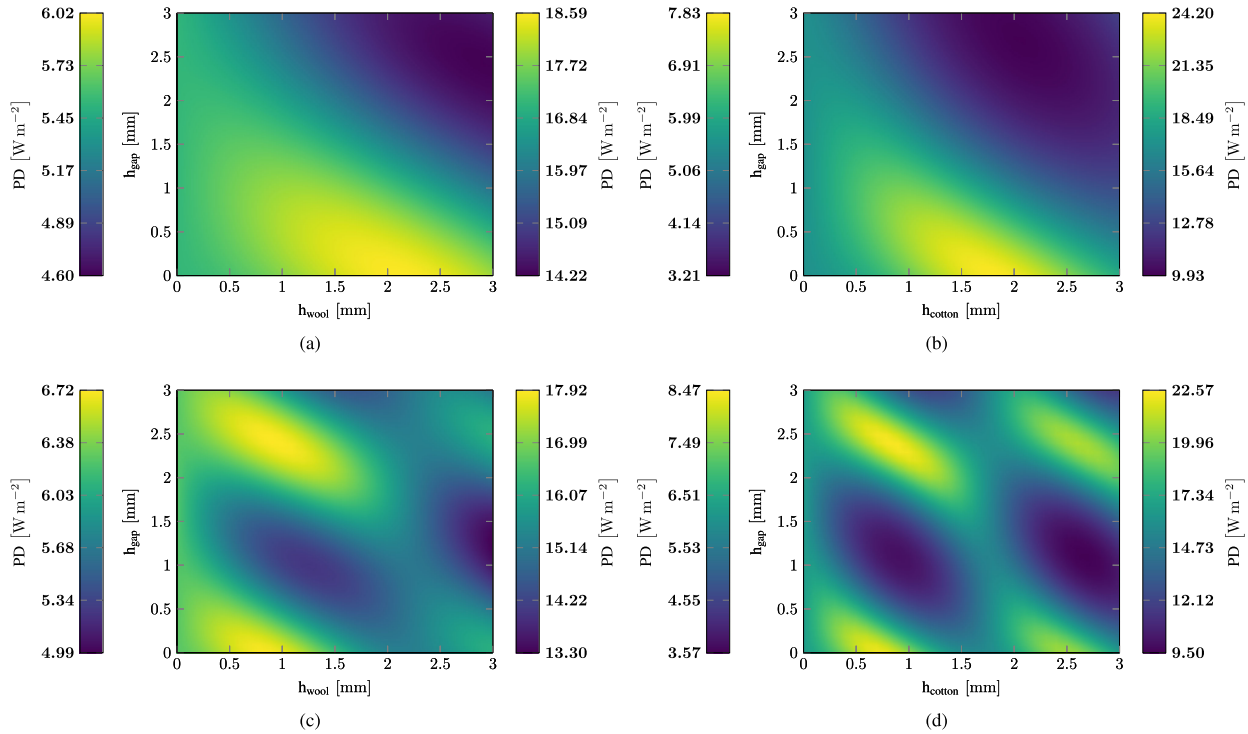

Fig. 6. Absorbed power density at 26 GHz: (a) wool and 26 GHz, (b) cotton and 60 GHz, (c) wool, and (d) cotton. The left and right colorbars on the left side refer to the frequency-independent and frequency-dependent limits of IPD, respectively.

$IPD = 30.90$ W m^{-2}). At 60 GHz, the highest PD is for 0.74 mm thick cotton (8.42 W m^{-2} and 22.43 W m^{-2} for $IPD = 10$ W m^{-2} and $IPD = 26.65$ W m^{-2}, respectively). The slightly higher value at 26 GHz than at 60 GHz when considering frequency-dependent limits is due to the fact that at 26 GHz the IPD limit is more elevated and losses in the textile are inferior at lower frequencies.

To consider other possible textile materials, the real part of the textile permittivity was varied in the 1–3 range. The imaginary part was kept equal to that of wool. The resulting PD at 26 GHz and 60 GHz are represented in Fig. 5. At both frequencies, the maximum PD is at $\varepsilon_r = 3$ and is equal to 9.11 W m^{-2} (for $h_{textile} = 1.49$ mm) and to 9.46 W m^{-2} (for $h_{textile} = 0.58$ mm) at 26 GHz and 60 GHz, respectively, for $IPD = 10$ W m^{-2}. Considering the frequency-dependent limits, the highest PD is 28.16 W m^{-2} at 26 GHz and 25.20 W m^{-2} at 60 GHz. As it was previously observed, at 60 GHz, due to increased electrical size of the textile compared to 26 GHz, two local maxima appear.

When accounting for an air gap between the textile and skin, the maximum PD does not occur at $h_{textile} = (2n+1)\lambda/4$ anymore, and depends on the air gap thickness (Fig. 6). Considering the frequency-independent IPD limits, the maximum PD is 6.02 W m^{-2} for the wool and 7.83 W m^{-2} for the cotton at 26 GHz, while at 60 GHz it reaches 6.73 W m^{-2} and 8.47 W m^{-2} for the wool and the cotton, respectively. These values are comparable to the maximum PD obtained for the configuration without an air gap between skin and textile.

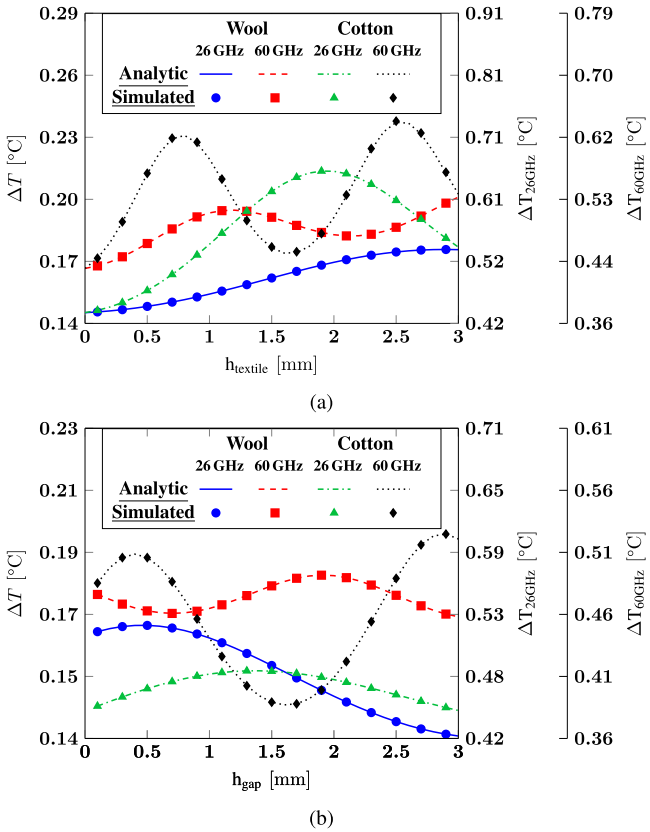

Fig. 7. Maximal steady-state temperature elevation in the skin layer at 26 GHz and 60 GHz (a) as a function of the textile layer thickness (wool or cotton) for $h_{gap} = 0$ mm and (b) as a function of the air gap thickness for $h_{wool} = 2$ mm and $h_{cotton} = 0.2$ mm. The left y axis refers to the frequency-independent IPD limits, while the two y axis on the right refer to the IPD frequency-dependent limits.

C. Heating

To evaluate the heating, the steady-state temperature rise inside the skin layer, reached after roughly 30–40 min of exposure, was calculated. This represents the worst case scenario, and the temperature rise during the transient heating is expected to be lower. Fig. 7(a) shows the temperature rise without an air gap as a function of the textile thickness. Presence of a textile in contact with skin increases heating. The highest temperature rise occurs for a textile thickness close to $(2n+1)\lambda/4$. Contrary to the trend of PD, the temperature increase at 60 GHz is higher for $h_{cotton} = 3/4\lambda$, compared to $h_{cotton} = \lambda/4$. In fact, a thicker textile reduces the thermal exchange between skin and air. The maximal temperature increase at steady-state, corresponding to these two configurations for the frequency-independent limits, is 0.21 °C at 26 GHz and 0.24 °C at 60 GHz, while for frequency-dependent limits it reaches 0.66 °C and 0.64 °C at 26 GHz and 60 GHz, respectively. Therefore the heating is up to 52% and 46% higher in presence of a textile at 26 GHz and 60 GHz, respectively.

With an air gap, the temperature was calculated for the textile thickness corresponding to the typical values, i.e. 0.2 mm for cotton and 2 mm for wool Fig. 7(b). In this case the maximum temperature rise at 26 GHz is 0.17 °C for $IPD = 10$ W m $^{-2}$ and 0.52 °C for $IPD = 30.90$ W m $^{-2}$. At 60 GHz the highest temperature increase is 0.2 °C for IPD $= 10$ W m $^{-2}$ and 0.53 °C for IPD $= 26.65$ W m^{-2}.

IV. Discussion and Conclusion

We investigated and quantified the impact of a textile layer on the electromagnetic power deposition and resulting heating in a stratified near-surface tissue model. In continuation to the previous studies [13]–[15], this work provides an insight into the PD variation and resulting heating, which are two fundamental parameters to evaluate the exposure above 6 GHz. A normally impinging plane wave was considered as a source. Note that an oblique incidence would result in a lower PD and temperature elevation [29]. Aiming at the worst case condition, the temperature elevation was investigated at steady-state. Our results show that the presence of a textile in direct contact with skin increases the absorbed power density up to 41.5% at 26 GHz and 34.4% at 60 GHz. This is due to the fact that it plays a role of a matching layer. The presence of an air gap between the textile and skin can decrease or increase the electromagnetic power deposition in the tissues depending on the air gap and textile thicknesses, and on the textile complex permittivity. Without an air gap between a textile and skin, the temperature rise increases compared to the bare skin (up to 52% at 26 GHz and 46% at 60 GHz). With an air gap and for the typical textile thicknesses, it ranges from -3.5% to 20.6% and from -11.1% to 20.9% at 26 GHz and 60 GHz, respectively. When considering the available bandwidths for 5G applications, i.e. 24.25–29.5 GHz (including n257, n258, and n261 bands) [30] and the 57–66 GHz band [31], the maximal PD in presence of a textile varies by at most 3.2% and 9.9%, respectively. These variations are of the same order of magnitude as the typical inter-individual variations. Validation of these conclusions using more realistic models constitutes one of the perspectives of this study.

Acknowledgment

The authors would like to thank Zain Haider for proofreading the article.

References

[1] "High five," *Nature Electronics*, vol. 3, no. 1, pp. 1–1, Jan. 2020.
[2] T. S. Rappaport, "Millimeter wave mobile communications for 5G cellular: It will work!," *IEEE Access*, vol. 1, pp. 335–349, 2013.
[3] International Commission on Non-Ionizing Radiation Protection (ICNIRP), "Guidelines for limiting exposure to electromagnetic fields (100 kHz to 300 GHz)," *Health Phys.*, vol. 118, no. 5, pp. 483–524, May 2020.
[4] International Electrical and Electronics Engineers (IEEE), "IEEE standard for safety levels with respect to human exposure to electric, magnetic, and electromagnetic fields, 0 Hz to 300 GHz," 2019.
[5] A. R. Guraliuc, M. Zhadobov, R. Sauleau, L. Marnat, and L. Dussopt, "Near-field user exposure in forthcoming 5G scenarios in the 60 GHz band," *IEEE Trans. Antennas Propag.*, vol. 65, no. 12, pp. 6606–6615, Dec. 2017.
[6] S. Kodera, J. Gomez-Tames, and A. Hirata, "Temperature elevation in the human brain and skin with thermoregulation during exposure to RF energy," *BioMedical Eng. OnLine*, vol. 17, no. 1, p. 1, Dec. 2018.
[7] G. Piro, P. Bia, G. Boggia, D. Caratelli, L. Grieco, and L. Mescia, "Terahertz electromagnetic field propagation in human tissues: A study on communication capabilities," *Nano Commun. Netw.*, vol. 10, pp. 51–59, Dec. 2016.

[8] L. Mescia, P. Bia, M. Chiapperino, and D. Caratelli, "Fractional calculus based FDTD modeling of layered biological media exposure to wideband electromagnetic pulses," *Electronics*, vol. 6, no. 4, p. 106, Nov. 2017.
[9] A. Christ, T. Samaras, E. Neufeld, and N. Kuster, "RF-induced temperature incerase in a stratified model of the skin for plane-wave exposure at 6–100 GHz," *Radiat. Protection Dosimetry*, vol. 188, no. 3, pp. 350–360, Jun. 2020.
[10] K. Sasaki, M. Mizuno, K. Wake, and S. Watanabe, "Monte Carlo simulations of skin exposure to electromagnetic field from 10 GHz to 1 THz," *Phys. Med. Biol.*, vol. 62, no. 17, pp. 6993–7010, Aug. 2017.
[11] M. C. Ziskin, S. I. Alekseev, K. R. Foster, and Q. Balzano, "Tissue models for RF exposure evaluation at frequencies above 6 GHz," *Bioelectromagnetics*, vol. 39, no. 3, pp. 173–189, Apr. 2018.
[12] M. Zhadobov, N. Chahat, R. Sauleau, C. Le Quement, and Y. Le Drean, "Millimeter-wave interactions with the human body: State of knowledge and recent advances," *Int. J. Microw. Wireless Technol.*, vol. 3, no. 2, pp. 237–247, Apr. 2011.
[13] A. R. Guraliuc, M. Zhadobov, G. Valerio, and R. Sauleau, "Enhancement of on-body propagation at 60 GHz using electro textiles," *IEEE Antennas Wireless Propag. Lett.*, vol. 13, pp. 603–606, 2014.
[14] A. R. Guraliuc, M. Zhadobov, G. Valerio, N. Chahat, and R. Sauleau, "Effect of textile on the propagation along the body at 60 GHz," *IEEE Trans. Antennas Propag.*, vol. 62, no. 3, pp. 1489–1494, Mar. 2014.
[15] O. Gandhi and A. Riazi, "Absorption of millimeter waves by human beings and its biological implications," *IEEE Trans. Microw. Theory Techn.*, vol. MTT-34, no. 2, pp. 228–235, Feb. 1986.
[16] P. Chitrphiromsri and A. V. Kuznetsov, "Modeling heat and moisture transport in firefighter protective clothing during flash fire exposure," *Heat Mass Transfer*, vol. -1, no. 1, pp. 1–1, Jun. 2003.
[17] C. Gabriel, "Compilation of the dielectric properties of body tissues at RF and microwave frequencies," Defense Technical Information Center, Fort Belvoir, VA, Tech. Rep., Jan. 1996.
[18] J. Luo, Y. Shao, X. Liao, J. Liu, and J. Zhang, "Complex permittivity estimation for cloths based on QPSO method over 40–50 GHz," *IEEE Trans. Antennas Propag.*, pp. 1–1, 2020.
[19] N. Rezgui, N. Bowring, Z. Luklinska, S. Harmer, and G. Ren, "Determination of the complex permittivity of textiles and leather in the 14–40 GHz millimetre-wave band using a free-wave transmittance only method," *IET Microw., Antennas Propag.*, vol. 2, no. 6, pp. 606–614, Sep. 2008.
[20] ITIS Foundation, "Database of Tissue Properties [Online],"
[21] W. E. Morton and J. W. S. Hearle, *Physical Properties of Textile Fibres*, 4th ed., ser. Woodhead Publishing in Textiles. Boca Raton, Fla.: CRC Press [u.a.], 2008, no. 68.
[22] D. Romeli, G. Barigozzi, S. Esposito, G. Rosace, and G. Salesi, "High sensitivity measurements of thermal properties of textile fabrics," *Polymer Testing*, vol. 32, no. 6, pp. 1029–1036, Sep. 2013.
[23] G. Havenith, K. Kuklane, J. Fan, and S. Hodder, "A database of static clothing thermal insulation and vapor permeability values of non-western ensembles for use in ASHRAE Standard 55, ISO 7730, and ISO 9920," *ASHRAE Trans*, vol. 121, p. 20, 2015.
[24] S. He, D. Huang, Z. Qi, H. Yang, Y. Hu, and H. Zhang, "The effect of air gap thickness on heat transfer in firefighters' protective clothing under conditions of short exposure to heat," *Heat Transfer Research*, vol. 43, no. 8, pp. 749–765, 2012.
[25] G. Song, S. Mandal, and M. Rossi, *Thermal Protective Clothing for Firefighters*, 2016.
[26] W. Kannuluik and E. Carman, "The temperature dependence of the thermal conductivity of air," *Australian Journal of Chemistry*, vol. 4, no. 3, p. 305, 1951.
[27] J. P. Holman, *Heat Transfer, 10th Edition*, 10th ed. New York: McGraw-Hill, 2010.
[28] M. Ziane, R. Sauleau, and M. Zhadobov, "Antenna/body coupling in the near-field at 60 GHz: Impact on the absorbed power density," *Appl. Sci.*, vol. 10, no. 21, p. 7392, Oct. 2020.
[29] K. Li, K. Sasaki, S. Watanabe, and H. Shirai, "Relationship between power density and surface temperature elevation for human skin exposure to electromagnetic waves with oblique incidence angle from 6 GHz to 1 THz," *Phys. Med. Biol.*, vol. 64, no. 6, p. 065016, Mar. 2019.
[30] European Telecommunications Standards Institute (ETSI), "5G; NR; user equipment (UE) radio transmission and reception; Part 2: Range 2 standalone (3GPP TS 38.101-2 version 15.3.0 Release 15)," Oct. 2018.
[31] European Telecommunications Standards Institute (ETSI)-, "Multiple-Gigabit/s radio equipment operating in the 60 GHz band; Harmonised standard covering the essential requirements of article 3.2 of Directive 2014/53/EU," Jul. 2017.

Giulia Sacco (Student Member, IEEE) received the B.S. and the M.S. degrees *(cum laude)* in biomedical engineering from Sapienza University of Rome, Rome, Italy, in 2015 and 2017, respectively. She is currently working toward the Ph.D. degree with Sapienza University of Rome. From April 2019 to September 2019, she was a Visiting Research with Stiching imec Eindhoven, The Netherlands. Since November 2019, she has been a Visiting Researcher with IETR (Institut d'Electronique et des Technologies du numrique), Rennes, France. Her scientific interests and research interests include the field of innovative biomedical applications of electromagnetic fields and radars for vital signs monitoring. She was the recipient of the Best Student Paper Award at Photonics & Electromagnetics Research Symposium (PIERS) 2019 and the Best Student Paper Award at the XXXIII General Assembly and Scientific Symposium (GASS) of the International Union of Radio Science (Union Radio Scientifique Internationale-URSI) 2020.

Stefano Pisa (Senior Member, IEEE) received the Electronic Engineering and Ph.D. degrees from the University of Rome "La Sapienza", Rome, Italy, in 1985 and 1988, respectively. In 1989, he was with the Department of Information Engineering, Electronics and Telecommunications (DIET), Sapienza University of Rome as a Researcher, where he has been an Associate Professor since 2001. He serves as a reviewer for various international journals. He has authored or coauthored more than 180 scientific papers. His research interests include the interaction between electromagnetic fields and biological systems, therapeutic and diagnostic applications of electromagnetic fields, medical applications of radar, and the modeling and design of MW circuits. He is a Senior Member of the IEEE Microwave Theory and Techniques Society, and a member of the Italian Society of Electromagnetics (SIEm).

Maxim Zhadobov (Senior Member, IEEE) received the M.S. degree in electromagnetics from the University of Nizhny Novgorod, Russia, in 2003, and the Ph.D. and Habilitation Diriger des Recherches degrees from the IETR (Institut d'Electronique et des Technologies du numerique), University of Rennes 1, France, in 2006 and 2016, respectively. He was a Postdoctoral Researcher with the Center for Biomedical Physics, Temple University, Philadelphia, PA, USA, until 2008, and then joined the French National Center for Scientific Research (CNRS). He is currently the Principal Investigator in biomedical electromagnetics with the IETR/CNRS and head of the WAVES Team, IETR. He coauthored five book chapters, five patents, more than 75 research papers in peer-reviewed international journals and 180 contributions to conferences and workshops. His scientific interests and research interests include in the field of innovative biomedical applications of electromagnetic fields and associated technologies. His review article in the *International Journal of Microwave and Wireless Technologies* has been the most cited paper in 2016–2020. A paper published by his research group in 2019 is in Journal Top 100 of Nature Scientific Reports. He has been involved in 23 research projects (12 as PI). He was the TPC Co-Chair of BioEM 2021, Honolulu, Hawaii and BioEM 2020, Oxford, U.K. He was a TPC member and/or session organizer at international conferences, including BioEM 2019, EuMW 2019, IEEE iWEM 2017, MobiHealth 2015–2017, BodyNets 2016, and IMWS-Bio 2014. He is an elected member of EBEA Council, member of IEEE TC95.4, and Vice-President of URSI France Commission K. He served as a Guest Editor of several Special Issues, including "Human Exposure in 5G and 6G Scenarios" of Applied Sciences and "Advanced Electromagnetic Biosensors for Medical, Environmental and Industrial Applications" of Sensors. He also served on review boards of more than 15 international journals and conferences, and has been acting as an expert at research councils worldwide. He received CNRS Medal in 2018, EBEA Award for Excellence in Bioelectromagnetics in 2015, and Brittany's Young Scientist Award in 2010. Since 2010, Ph.D. students he supervised received seven national scientific awards and five awards from the Bioelectromagnetics Society, URSI and IEEE Antennas and Propagation Society.